Journal of Power Sources 196 (2011) 9429–9436

Contents lists available at ScienceDirect

Journal of Power Sources

journal homepage: www.elsevier.com/locate/jpowsour

Percolation theory in SOFC composite electrodes: Effects of porosity and particle size distribution on effective properties

A. Bertei*, C. Nicolella

Department of Chemical Engineering, University of Pisa, Via Diotisalvi 2, 56126 Pisa, Italy

ARTICLE INFO

Article history:
Received 26 January 2011
Received in revised form 18 April 2011
Accepted 22 June 2011
Available online 1 July 2011

Keywords:
Percolation theory
SOFC
Pore formers
Polydisperse powders
Three-phase boundary length
Effective properties

ABSTRACT

A percolation model, accounting for polydispersion of powders and presence of pore formers (i.e. porosity), is presented to predict effective properties of composite electrodes for solid oxide fuel cells, such as the three-phase boundary length and the mean hydraulic radius. Porosity affects both numbers of contacts (so probabilities of connection) and number of particles per unit volume. Both these effects, together with granulometric distribution, are accounted for the estimation of effective properties. As a consequence, the theory can predict numbers of contacts, coordination numbers and therefore effective properties of the electrode for multicomponent polydisperse mixtures.

Model simulations show that the three-phase boundary length sharply decreases as porosity increases while the effects of polydispersion of powders are less pronounced, although significant, suggesting that these features should be considered in SOFC electrode models.

1. Introduction

Porous composite electrodes are used in the architecture of solid oxide fuel cells (SOFCs) [1,2]. A composite electrode is a sintered random packing of electron-conducting particles and ion-conducting particles where electrochemical reactions of oxidation or reduction occur. As an example, a typical composite cathode is a mixture of lanthanum-doped strontium manganite (LSM) as electronic conductor and yttria-stabilized zirconia (YSZ) as ionic conductor [3]. The charge transfer step is considered to take place where the reaction constituents (i.e. electrons, ions and chemical species) can coexist. These sites are the three-phase boundaries (TPBs) where the distinct phases, transporting the three participating species, meet.

The electrode performance is strictly dependent on its morphology. In particular the extension of the reactive zone, the effective conductivities of the phases and the morphological properties related to the gas phase are function of particle size, composition, porosity and sintering conditions. As a consequence, the engineered design of electrodes requires understanding and optimization of their morphology [3,4].

The main aim of studying the electrode morphology is to predict the effective functional properties (e.g. the mean pore diameter, the effective conductivity of phases, the three-phase boundary length) starting from measurable parameters such as the granulometric distribution of the powders and their composition. Methods for characterizing electrode morphology can be broadly classified as: (i) experimental techniques, (ii) computer simulations of random packings and (iii) predictions based on percolation theory.

Microstructural parameters can be measured on existing samples by image analysis on scanning electron microscopy (SEM) images or by other specific experimental techniques (e.g. measurements of effective conductivity or BET adsorption measurements). The morphology of the packing can be reconstructed (e.g. by ion beam SEM) and analyzed [5–7]. These techniques allow correlations of electrode properties to powder characteristics, but they rely on the resolution of the image and/or phase identification, making analysis of small features difficult and, in some cases, uncertain.

Composite electrodes are often modeled as random mixtures of spherical particles containing at least two solid phases: electron-conducting phase and ion-conducting phase [8–10]. The electrode structure can be reproduced by using a packing algorithm and morphological parameters are evaluated on the simulated packing [11–13]. Despite crude simplifications, this method is faster and may be more accurate than experimental techniques since it is not affected by experimental and image-processing uncertainties.

Microstructural properties can also be evaluated by using a stochastic theory regarding the particle arrangement in the

* Corresponding author. Tel.: +39 3334687172; fax: +39 (0)502217866.
E-mail addresses: antonio.bertei@for.unipi.it, berteiantonio@libero.it (A. Bertei).

0378-7753/$ – see front matter © 2011 Elsevier B.V. All rights reserved.
doi:10.1016/j.jpowsour.2011.06.087

packing, i.e. by using percolation theory. This mathematical tool has been widely used to describe morphological properties of random packings of solid particles, in particular in SOFC modeling [8,9,14], due to its easier applicability. Unlike simulation methods based on numerical packing generation, it is a predictive method, since functional properties are obtained directly from measurable starting input parameters, such as particle size and powder composition.

Percolation theory relies on the prediction of coordination numbers of particles, i.e. the number of contacts made by a particle with its neighboring particles. Functional morphological properties are predicted starting from the evaluation of coordination numbers. Several percolation models have been developed [14–16], based on different basic relationships used to calculate coordination numbers as a function of particle size and composition. In a previous paper [17] the authors showed a critical comparison of existing percolation theories and proposed a new method based on the improvement of the Suzuki and Oshima theory [15] to obtain a better agreement with simulated and experimental results and an extension of the theory to multicomponent polydisperse powders. As the basis for the development presented in this work, the essential features of the new method are recalled in the background of the theoretical section (see Section 2.1).

The present paper develops an extension of the previous theory to systems where porosity is controlled by addition of pore formers in the particle mixture. Pore formers are particles of materials which decompose at high temperatures, mixed with the powders before sintering in order to increase the porosity of the packing after sintering. Typical pore former materials are starch [18,19] and graphite [20,21] which burn in oxidizing atmosphere during the sintering. Although commonly used in electrodes fabrication, pore formers have not considered yet in percolation theories.

The focus of this paper is then on the application of the new percolation model to predict effective properties for composite electrodes of SOFCs, showing in particular the effects of both the presence of pore formers and the polydispersion of powders. In the theoretical section, the percolation model is first presented (Section 2.1) and then the extension to consider pore former effects is developed (Section 2.2). After a section dedicated to analyze if overlapping effects affect the percolation theory estimations (Section 2.3), the derivation of effective functional properties based on percolation theory is shown (Section 2.4). Model outcomes are specifically discussed in chapter 3.

2. Theory

2.1. Background

This section summarizes the key features of the percolation model previously developed [17]. This model was compared and validated with other percolation models [14–16] over a wide range of particle sizes and compositions. Despite in electrode fabrication only two conducting phases are used (i.e. electron-conducting and ion-conducting), also a third solid phase is here considered, which may represent pore former particles (as discussed in Section 2.2) or other types of particles.

Let us consider a ternary polydisperse mixture of rigid spherical particles, namely k, l and f. The packing is characterized by a distribution of m_k particle sizes for k-particles (i.e. different radii $r_{k1}, r_{k2} \ldots r_{km_k}$), m_l for l-particles and m_f for f-particles. For a generic kind of hi-particles (h = k, l or f while i varies from 1 to m_k, m_l or m_f), characterized by a radius r_{hi}, basic definitions of ratio of radii with another generic kind of gj-particles (g = k, l or f while j varies from 1 to m_k, m_l or m_f), numerical, volumetric and surface-specific fractions before sintering are as follows:

$$P_{hi,gj} = \frac{r_{hi}}{r_{gj}} \tag{1}$$

$$\zeta_{hi} = \frac{n^v_{hi}}{\sum_{j=1}^{m_k} n^v_{kj} + \sum_{j=1}^{m_l} n^v_{lj} + \sum_{j=1}^{m_f} n^v_{fj}} = \frac{\psi_{hi}/r^3_{hi}}{\sum_{j=1}^{m_k} \psi_{kj}/r^3_{kj} + \sum_{j=1}^{m_l} \psi_{lj}/r^3_{lj} + \sum_{j=1}^{m_f} \psi_{fj}/r^3_{fj}} \tag{2}$$

$$\psi_{hi} = \frac{\zeta_{hi} r^3_{hi}}{\sum_{j=1}^{m_k} \zeta_{kj} r^3_{kj} + \sum_{j=1}^{m_l} \zeta_{lj} r^3_{lj} + \sum_{j=1}^{m_f} \zeta_{fj} r^3_{fj}} \tag{3}$$

$$S_{hi} = \frac{\zeta_{hi} r^2_{hi}}{\sum_{j=1}^{m_k} \zeta_{kj} r^2_{kj} + \sum_{j=1}^{m_l} \zeta_{lj} r^2_{lj} + \sum_{j=1}^{m_f} \zeta_{fj} r^2_{fj}} = \frac{\psi_{hi}/r_{hi}}{\sum_{j=1}^{m_k} \psi_{kj}/r_{kj} + \sum_{j=1}^{m_l} \psi_{lj}/r_{lj} + \sum_{j=1}^{m_f} \psi_{fj}/r_{fj}} \tag{4}$$

where n^v_{hi} represents the number of hi-particles per unit volume.

The packing homogeneity depends on the values of $P_{hi,gj}$. For a couple of particles hi-gj, segregation occurs if the smaller particles, for example hi-particles, can pass through the void left by three larger particles, for example gj-particles, in contact with each other [22]. Indeed, by joining the centers of bigger gj-particles to form an equilateral triangle, by geometrical considerations the void left in the middle can contain at the maximum a particle of radius $(2/\sqrt{3} - 1)r_{gj}$: if r_{hi} is higher, segregation cannot occur. This consideration could be repeated if hi-particles are bigger than gj-particles, providing a restriction on r_{gj} as $r_{gj} > (2/\sqrt{3} - 1)r_{hi}$. Thus, a sufficient condition to avoid segregation for the multicomponent polydisperse mixture is given if $P_{hi,gj}$ is in the range from $P_{\min} = 2/\sqrt{3} - 1$ to $P_{\max} = (2/\sqrt{3} - 1)^{-1}$ for each couple of particles hi-gj.

The generic average number of contacts between hi- and gj-particles $Z_{hi,gj}$, i.e. the number of gj-particles in contact with a hi-particle, is proposed to be proportional to surface-specific fraction of gj-particles as in Suzuki and Oshima model [15]:

$$Z_{hi,gj} = S_{gj} Z_{hi,gj}\big|_{\zeta_{gj}\to 1} \tag{5}$$

$Z_{hi,gj}\big|_{\zeta_{gj}\to 1}$ represents the limit of the number of contacts that a hi-particle makes with gj-particles in a binary hi-gj mixture when there are only a few hi-particles in the packing. It depends only on the ratio of radii $P_{hi,gj}$ and it is estimated as follows:

$$Z_{hi,gj}\big|_{\zeta_{gj}\to 1} = \begin{cases} \dfrac{3(2-\sqrt{3})(P_{hi,gj}+1)}{[1+P_{hi,gj}-(P_{hi,gj}(P_{hi,gj}+2))^{0.5}]} & \text{if } P_{hi,gj} \geq 1 \\ \dfrac{3(2-\sqrt{3})(P^{-1}_{hi,gj}+1)}{[1+P^{-1}_{hi,gj}-(P^{-1}_{hi,gj}(P^{-1}_{hi,gj}+2))^{0.5}]P^{-2}_{hi,gj}} & \text{if } P_{hi,gj} < 1 \end{cases} \tag{6}$$

Eq. (6) represents the improvement of Suzuki and Oshima theory as extensively discussed in [17].

For a generic hi-particle, the number of contacts between hi and all kinds of g-particles $Z_{hi,g}$, where g represents k-, l- or f-particles, is calculated as the summation of the number of contacts that a hi-particle makes with other gj-particles:

$$Z_{hi,g} = \sum_{j=1}^{m_g} Z_{hi,gj} \quad \text{with } g = \text{k, l or f} \tag{7}$$

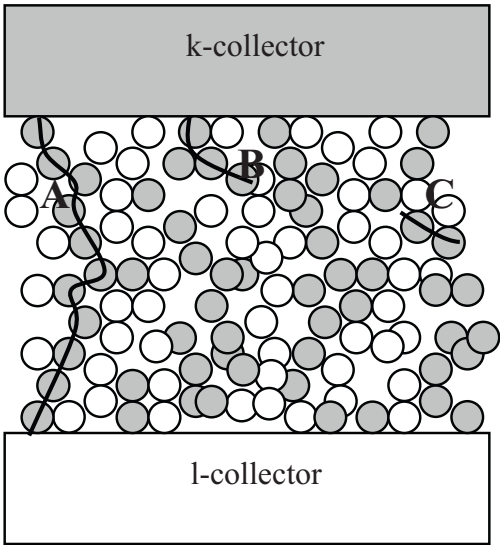

Fig. 1. Illustration of a composite electrode with A-(i.e. entirely connected), B-(i.e. partly connected) and C-(i.e. isolated) clusters indicated for k-phase.

The average coordination number of hi-particles (Z_{hi}) is then defined as the sum of the average number of contacts that hi-particles make with k-, l- and f-particles:

$$Z_{hi} = Z_{hi,k} + Z_{hi,l} + Z_{hi,f} \tag{8}$$

The overall average number of contacts for all h-particles $Z_{h,h}$, i.e. the average number of contacts that a h-particle makes with other homologue h-particles, is proposed to be equal to the total number of h–h contacts in the mixture divided by the total number of h-particles as already proposed by Chen et al. [14]:

$$Z_{h,h} = \frac{\sum_{i=1}^{m_h} \zeta_{hi} Z_{hi,h}}{\sum_{i=1}^{m_h} \zeta_{hi}} \quad \text{with } h = \text{k, l or f} \tag{9}$$

As shown in Fig. 1, a percolating (or A-) cluster is a cluster of particles of the same type that extends through the entire thickness of the electrode. On the other hand, B- and C-clusters are not entirely connected because B-clusters are short networks connected only to the respective collector while C-clusters are completely isolated [9]. The probability of connection p_h, i.e. the probability that a generic h-particle belongs to a percolating cluster of the same kind of particles, depends only on the overall average number of contacts among h-particles $Z_{h,h}$ [16]. The probability of connection p_h is then calculated as [17]:

$$p_h = 1 - \left(\frac{4.236 - Z_{h,h}}{2.472} \right)^{3.7} \tag{10}$$

Eq. (10) can also be used to individuate percolation thresholds, i.e. the minimum volume fraction of particles which determines percolating clusters of particles of the same type. In particular, taking generically h-particles as reference, when p_h equals 0 (i.e. for $Z_{h,h} = 1.764$) in the mixture there are no more percolating clusters of h-particles. It means that the h-phase is no more connected through the whole thickness of the packing and, as a result, the effective conductivity of this phase approaches 0.

2.2. Extension of the percolation model including pore formers effects

The percolation theory presented in the previous section is extended to take into account the presence of pore formers in the particle mixture. Pore former particles are not present in the final structure because they decompose during the sintering.

In a ternary mixture of k-, l- and f-particles as considered in Section 2.1, where f-particles represent pore former particles, we assume that after sintering f-particles disappear leaving holes of the same shape and dimension of the particle of pore former that occupied that position before sintering. The resulting structure, obtained after sintering, will contain only k- and l-particles. It is then assumed that size and position of each k- and l-particle do not change during the sintering. This assumption is valid only if the structure does not collapse during the sintering. Structure collapse may reasonably occur for high volume fractions of pore formers (such as to create porosity higher than 50–60%) or if pore former particles are much bigger than k- and l-particles, resulting in big holes whose surrounding structure is mechanically unstable. Even when pore former particles are much smaller than k- and l-particles the structure may collapse since the smaller f-particles surround other coarser particles isolating them [23]: during the sintering, the gradual disappearance of pore former particles brings the particles placed above them to come down.

In order to calculate numbers of contacts, Eqs. (1)–(4) remain valid for all the types of particles (i.e. k, l and f) because they represent the ratio or radii and numerical, volumetric and surface-specific fractions before sintering. These quantities still continue to have a physical meaning after sintering since f-particles (and their correlated quantities) represent the spherical holes left in the structure. Nevertheless, after sintering Eqs. (5)–(7) and (9)–(10) continue to make sense only for k- and l-particles (i.e. for h and g equal to k or l), despite numerical and surface-specific fractions involved in calculations must be determined by using Eqs. (1)–(4) where pore formers are considered. Numbers of contacts regarding f-particles do not have any physical meaning after sintering, although f-particles affect the determination of numbers of contacts of k- and l-particles since they represent missing particles. Coordination numbers for k- and l-particles can be calculated by using Eq. (8), nevertheless the contacts with f-particles must be ignored:

$$Z_{ki} = Z_{ki,k} + Z_{ki,l} \tag{11}$$

$$Z_{li} = Z_{li,k} + Z_{li,l} \tag{12}$$

Pore formers affect not only the calculation of numbers of contacts but also the number of particles per unit volume. The final porosity ϕ_g^{fin} of the structure (i.e. after sintering) can be calculated as:

$$\phi_g^{fin} = \phi_g^{in} + \phi_g^{f} \tag{13}$$

where ϕ_g^{in} is the initial porosity of the mixture (i.e. before sintering) when all k-, l- and f-particles are present. ϕ_g^{f} is the fraction of porosity added by pore formers calculated as:

$$\phi_g^{f} = n^{v,bs} \sum_{i=1}^{m_f} \zeta_{fi} (4/3) \pi r_{fi}^3 \tag{14}$$

where $n^{v,bs}$ is the number of particles (k, l and f) per unit volume (voids included) before sintering estimated as:

$$n^{v,bs|} = \frac{1 - \phi_g^{in}}{\sum_{i=1}^{m_k} \zeta_{ki} (4/3) \pi r_{ki}^3 + \sum_{i=1}^{m_l} \zeta_{li} (4/3) \pi r_{li}^3 + \sum_{i=1}^{m_f} \zeta_{fi} (4/3) \pi r_{fi}^3} \tag{15}$$

The number of particles per unit volume after sintering $n^{v,as}$ is calculated as:

$$n^{v,as} = n^{v,bs} \left(\sum_{i=1}^{m_k} \zeta_{ki} + \sum_{i=1}^{m_l} \zeta_{li} \right) \tag{16}$$

The initial porosity ϕ_g^{in} depends on composition and granulometric distribution of powders before sintering but this relationship is not well known for multicomponent mixtures. Thus, if no particular measurement is available, a very rough estimation is $\phi_g^{in} = 0.36$, i.e. the porosity of a random close packing of monosized spheres of the same type [16,24–26]. In general, for binary mixtures of monosized (i.e. not polydisperse) particles with different radii, initial porosity can be evaluated with more accuracy as reported by Ben Aim and Le Goff [27].

2.3. Overlapping of particles

In percolation theory, particles are considered as spheres that do not overlap as they are rigid. On the other hand, in the manufactory of electrodes for SOFCs, particles are compressed and sintered. Then, assuming for instance that before sintering particles are spherical, after that operation we should expect that their shape shows overlapping regions. This implies that some properties of the packing, in particular numbers of contacts and coordination numbers of particles but also the number of particles per unit volume, could differ from the estimation made by assuming particles as rigid spheres.

The discrepancy between the properties of the sintered packing (i.e. with overlapping) and the modeled packing as considered by percolation theory (i.e. without overlapping) increases when contact angles among particles increase. The graphical definition of contact angles between a k- and a l-particle (i.e. θ_{kl} and θ_{lk}) is reported in Fig. 2.

In order to estimate the effects of overlapping at least on the number of particles per unit volume, let us consider a binary randomly packed mixture of k- and l-particles not polydisperse. As already mentioned by Janardhanan et al. [28], we can assume that:

1. Particles are spherical before sintering
2. The sintering process creates overlapping regions among particles characterized by mean contact angles θ_{kk}, θ_{kl}, θ_{lk} and θ_{ll}
3. After sintering particles keep quite the same position, same radii r_k and r_l and the spherical shape except in the overlapping region: the contact region between two particles is a perfect circle of radius $r_k \cdot \sin\theta_{kl} = r_l \cdot \sin\theta_{lk}$
4. Presence of overlapping regions made by three or more particles is neglected

We can calculate the fraction of volume lost in each kind of contact. We call $V_i^{lost,ij}$ the volume of a generic i-particle lost in a contact i-j (characterized by an angle θ_{ij}). According to Fig. 2, the lost volume is equal to the volume of a spherical segment of one base with height $r_i \cdot (1 - \cos\theta_{ij})$, so we obtain:

$$\begin{cases} V_k^{lost,kl} = \dfrac{\pi}{3} r_k^2 (1-\cos\theta_{kl})^2 \left[3r_k - r_k(1-\cos\theta_{kl})\right] \\ V_k^{lost,kk} = \dfrac{\pi}{3} r_k^2 (1-\cos\theta_{kk})^2 \left[3r_k - r_k(1-\cos\theta_{kk})\right] \\ V_l^{lost,lk} = \dfrac{\pi}{3} r_l^2 (1-\cos\theta_{lk})^2 \left[3r_l - r_l(1-\cos\theta_{lk})\right] \\ V_l^{lost,ll} = \dfrac{\pi}{3} r_l^2 (1-\cos\theta_{ll})^2 \left[3r_l - r_l(1-\cos\theta_{ll})\right] \end{cases} \quad (17)$$

with the constraint (see point 3 mentioned above):

$$r_k \sin\theta_{kl} = r_l \sin\theta_{lk} \quad (18)$$

that links together θ_{kl} and θ_{lk}.

Assuming that percolation properties of the mixture can be estimated by using percolation theory described in Section 2.1 although particles are not rigid spheres, the total volume lost in the contacts for each particle, k or l, is:

$$V_k^{lost} = Z_{k,l} V_k^{lost,kl} + Z_{k,k} V_k^{lost,kk} \quad (19)$$

$$V_l^{lost} = Z_{l,k} V_l^{lost,lk} + Z_{l,l} V_l^{lost,ll} \quad (20)$$

Thus, the effective volumes of the particles, V_k^{eff} and V_l^{eff}, are:

$$V_k^{eff} = (4/3)\pi r_k^3 - V_k^{lost} \quad (21)$$

$$V_l^{eff} = (4/3)\pi r_l^3 - V_l^{lost} \quad (22)$$

These relationships are useful to calculate the total number of particles per unit volume (voids included) with overlapping regions $n^{v,overlap}$:

$$n^{v,overlap} = \frac{1 - \phi_g^{in}}{\zeta_k V_k^{eff} + (1-\zeta_k) V_l^{eff}} \quad (23)$$

If $\theta_{ij} > 0$, $n^{v,overlap}$ will be higher than the value of $n^{v,bs}$ that we could calculate without considering overlapping effects as in Eq. (15).

For reasonable contact angles, i.e. $\theta_{kk} = \theta_{ll} = \max(\theta_{kl}, \theta_{lk}) \leq 15^\circ$ as commonly accepted in modeling works [8,9,14], the errors that we make on $n^{v,overlap}$ if we do not consider the overlapping effects (i.e. using $(4/3)\pi r_i^3$ instead of V_i^{eff}) will be less than 0.52% (the worst situation is represented by a binary mixture of k- and l-particles of the same size). It means that overlapping effects are negligible in the calculation of $n^{v,overlap}$; secondarily, it could mean that also the approximation of the mixture as a packing of rigid spheres is reasonable, so we can estimate coordination numbers of particles and other properties by using the relationships of percolation theory presented in Sections 2.1 and 2.2 even if particles are partly overlapped.

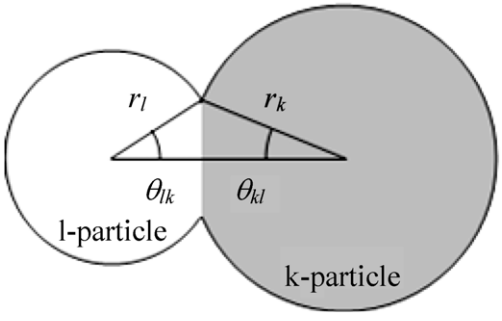

Fig. 2. Overlapping k- and l-particle, definition of contact angles.

2.4. Calculation of functional parameters

As far as modeling of electrodes for SOFCs is concerned, the most relevant morphological parameters are the three-phase boundary (TPB) length per unit volume λ_{TPB}^v, the contact area between connected k- and l-particles per unit volume a_{kl}^v, the surface area exposed by k- (or l-) particles to gas phase per unit volume a_k^v (or a_l^v) and the mean hydraulic radius R_h for the description of transport of gaseous products or reagents. The method proposed for the estimation of these parameters is presented in the following.

2.4.1. TPB length

When considering two types of conducting particles, k and l (e.g. k, electron-conducting phase, l, ion-conducting phase), the TPB is the contact perimeter between overlapping k- and l-particles. The third phase is the gas phase, generally assumed entirely connected (i.e. we can connect two generic points of the gas phase passing

only within the gas phase) for porosity higher than 25% [11]. At the TPB, electrons, ions and chemical species can simultaneously coexist. A k-l contact will be active for the charge-transfer reaction only if the k-particle belongs to a k-path connected to the k-collector and the l-particle to a l-path connected to the l-collector. Only in this situation reaction can occur at the TPB, e.g. in a cathode electrons flow from the electrode interconnect to the TPB to react with gaseous oxygen while oxygen ions flow from the reaction site at TPB to the dense electrolyte. The contributions of B-clusters (i.e. contacts between A-B, B-A or B-B clusters of different kinds, see Fig. 1) can generally be neglected, because, within percolation thresholds, their length is very low when the thickness of the electrode is reasonably big if compared with mean particle size [9]. In this case, only the contacts among particles belonging to A-clusters are taken into account.

The TPB length per unit volume is calculated starting from the TPB length per ki-lj contact $2\pi r_{ij}^c$, i.e. the contact perimeter, where r_{ij}^c is the neck radius of the circle formed by the ki-lj contact, calculated as:

$$r_{ij}^c = \min(r_{ki}, r_{lj})\ \sin(\theta_{ij}^c) \tag{24}$$

coupled with the definition of the contact angle θ_{ij}^c:

$$\theta_{ij}^c = \max(\theta_{ki,lj}, \theta_{lj,ki}) \tag{25}$$

The neck radius is calculated by referring to the smaller particle between ki and lj, i.e. by using the minimum particle radius between r_{ki} and r_{lj} and the maximum contact angle between $\theta_{ki,lj}$ and $\theta_{lj,ki}$.

The TPB length per unit volume is calculated through the following procedure:

1. The contact perimeter $2\pi r_{ij}^c$ is multiplied by the number of ki-lj contacts per unit volume, equal to $n^{v,bs}\zeta_{ki}Z_{ki,lj}$
2. The sum is extended to the $m_k \cdot m_l$ couples of contacts between k- and l-particles
3. Only particles belonging to connected clusters are considered by multiplying by p_k and p_l

Accordingly, the TPB length per unit volume is calculated as:

$$\lambda_{TPB}^v = n^{v,bs} p_k p_l 2\pi \sum_{i=1}^{m_k} \left(\zeta_{ki} \sum_{j=1}^{m_l} Z_{ki,lj} r_{ij}^c \right) \tag{26}$$

In particular, in Eq. (26) ζ_{ki} are the numerical fractions before sintering (i.e. considering also the presence of pore former particles) and $n^{v,bs}$, $Z_{ki,lj}$, p_k and p_l are calculated according to the relationships presented in Sections 2.1 and 2.2.

All the contact angles θ_{ij}^c (i.e. $m_k \cdot m_l$ parameters) must be assigned. It is reasonable to assume a single value for all of them and call it θ: in this situation Eq. (26) is similar to the expression already proposed by Chen et al. [14]. According to the considerations formulated above in Section 2.3, θ must be assumed in the order of 15° or less in order to apply the relationships of percolation theory. Other values of θ could be used, referred to different sintering conditions, but for big contact angles (i.e. $\theta > 30°$) particles are no more spherical, so percolation theory cannot be used.

2.4.2. Contact area

In a similar way, we can evaluate a_{kl}^v, i.e. the contact area between connected k- and l-particles per unit volume. The calculation of a_{kl}^v is similar to that of λ_{TPB}^v, only, instead of considering the contact perimeter $2\pi r_{ij}^c$ for each contact ki-lj, we take into account the contact area $\pi(r_{ij}^c)^2$:

$$a_{kl}^v = n^{v,bs} p_k p_l \pi \sum_{i=1}^{m_k} \left(\zeta_{ki} \sum_{j=1}^{m_l} Z_{ki,lj} (r_{ij}^c)^2 \right) \tag{27}$$

This last parameter characterizes reaction sites if the reaction takes place in the whole surface of contact between k- and l-particles instead of the contact perimeter.

2.4.3. Surface area

The total surface area exposed by k-particles to gas phase per unit volume a_k^v has a role concerning adsorption (or desorption) of substances from gas phase to k-particles. It is calculated by multiplying the total number of particles per unit volume before sintering $n^{v,bs}$ with the surface area of a ki-particle $4\pi r_{ki}^2$ and extending the summation to the m_k particle sizes:

$$a_k^v = 4\pi n^{v,bs} \sum_{i=1}^{m_k} \zeta_{ki} r_{ki}^2 \tag{28}$$

Eq. (28) can be applied also for l-particles. The expression takes into account the total external surface of k-particles without considering the fraction of surface lost in contacts. Considering contact angles of 15°, due to the fraction of surface lost in contacts, Eq. (28) overestimates a_k^v in the order of 11.4% in the worst case of a binary mixture of monosized k- and l-particles with $r_k = r_l$ without pore formers.

2.4.4. Hydraulic radius

Referring to the gas phase, the main parameter is the mean hydraulic radius R_h, estimated according to Bird et al. [29] as the ratio of the volume available for gas passage per unit volume, i.e. the final porosity ϕ_g^{fin}, and the total solid surface exposed to gas phase per unit volume, equal to the sum of a_k^v and a_l^v both calculated according to Eq. (28). By this definition, the hydraulic radius is calculated as:

$$R_h = \frac{\phi_g^{fin}}{4\pi n^{v,bs} \left(\sum_{i=1}^{m_k} \zeta_{ki} r_{ki}^2 + \sum_{i=1}^{m_l} \zeta_{li} r_{li}^2 \right)} \tag{29}$$

Since the fractions of surface lost in contacts are not considered in Eq. (29), as previously explained for a_k^v, R_h is underestimated in the order of 10.2% as maximum for contact angles of 15°. By definition, the mean diameter of pores is equal to 4 times the hydraulic radius.

3. Results and discussion

The model outcomes are the functional parameters λ_{TPB}^v, a_{kl}^v, a_k^v and R_h, calculated as described in the theoretical section (Section 2.4). In order to illustrate the model potentiality, functional parameters are calculated for several case-studies in different conditions to explain the role of starting input parameters (i.e. radii of particles, composition, porosity, etc.) on final morphological results. In particular, special attention is taken in illustrating the effects of porosity and of polydispersion of particles as the new features introduced by the model. All results are referred to $\theta = 15°$, i.e., in an accurate notation, $\theta = \theta_{kk} = \theta_{ll} = \theta_{ij}^c = 15°$. In the following, for numerical and volumetric compositions after sintering we mean:

$$\zeta_{hi}^{as} = \frac{\zeta_{hi}}{\sum_{i=1}^{m_k} \zeta_{ki} + \sum_{i=1}^{m_l} \zeta_{li}} \text{ and } \zeta_k^{as} = \sum_{i=1}^{m_k} \zeta_{ki}^{as},\ \zeta_l^{as} = \sum_{i=1}^{m_l} \zeta_{li}^{as} \tag{30}$$

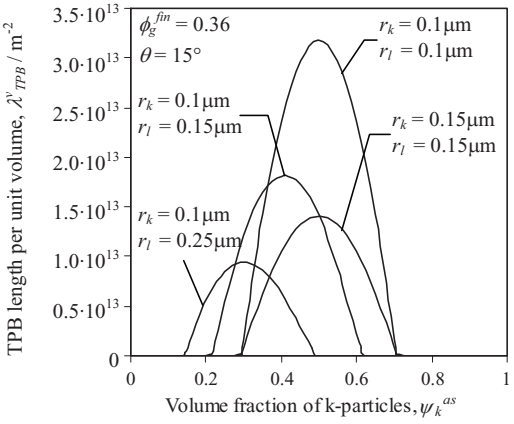

Fig. 3. TPB length per unit volume as a function of volumetric fraction of k-particles at different radii of particles for a binary not polydisperse mixture without pore formers ($\phi_g^{fin} = 0.36$, $\theta = 15°$).

$$\psi_{hi}^{as} = \frac{\psi_{hi}}{\sum_{i=1}^{m_k}\psi_{ki} + \sum_{i=1}^{m_l}\psi_{li}} \text{ and } \psi_k^{as} = \sum_{i=1}^{m_k}\psi_{ki}^{as},\ \psi_l^{as} = \sum_{i=1}^{m_l}\psi_{li}^{as} \quad (31)$$

for k- and l-phases (i.e. h = k or l) where ζ_{hi} and ψ_{hi} are, respectively numerical and volumetric fractions before sintering as already defined in the theoretical section (Section 2.1).

3.1. Particle size

Let us consider a binary mixture of monosized (not polydisperse) particles without pore formers; we assume for simplicity a constant final porosity of 36% for each composition and particle size ratio. Fig. 3 shows λ^v_{TPB} as a function of ψ_k^{as} for several radii of particles for $\theta = 15°$. When particles have the same radius, λ^v_{TPB} reaches a maximum at $\psi_k^{as} = 0.5$ and approaches 0 at the percolation thresholds. For a given composition, bigger particles yield lower values of λ^v_{TPB} than smaller particles. If l-particles are bigger than k-particles, the compositions where λ^v_{TPB} approaches 0 and at which λ^v_{TPB} is maximum move towards lower ψ_k^{as} since bigger particles (l) percolate worse than smaller particles (k) [23]. Note also that the width of the range of composition at which λ^v_{TPB} is not zero decreases as the ratio of radii $P_{k,l}$ is not 1.

3.2. Porosity

Fig. 4 shows in solid lines λ^v_{TPB} as a function of ψ_k^{as} for different porosities for a ternary not polydisperse mixture of particles with $r_k = r_l = r_f = 0.1\,\mu m$, where f-particles represent pore former particles; $\theta = 15°$ is used. When porosity increases, λ^v_{TPB} decreases and the range of compositions corresponding to $\lambda^v_{TPB} > 0$ becomes smaller.

The main feature of our percolation model is that the presence of pore formers has a double effect on λ^v_{TPB}: first it enters in the calculation of the numbers of contacts and connection probabilities, then it affects the calculation of number of particles per unit volume after sintering (Eq. (16)). In other percolation models [9,14], whose results are represented in Fig. 4 as dotted lines, the first effect is ignored, yielding an overestimation of TPB length and of the range where $\lambda^v_{TPB} > 0$ when pore formers are used. Provided that it is reasonable that pore formers reduce the number of contacts between k- and l-particles, our percolation model appears more reliable than other presented in Fig. 4.

Porosity has also effects on the mean hydraulic radius R_h. Fig. 5 shows R_h as a function of composition for different porosities with $r_f = 0.1\,\mu m$, $r_k = 0.1\,\mu m$ and $r_l = 0.15\,\mu m$ and with $\theta = 15°$. Initial

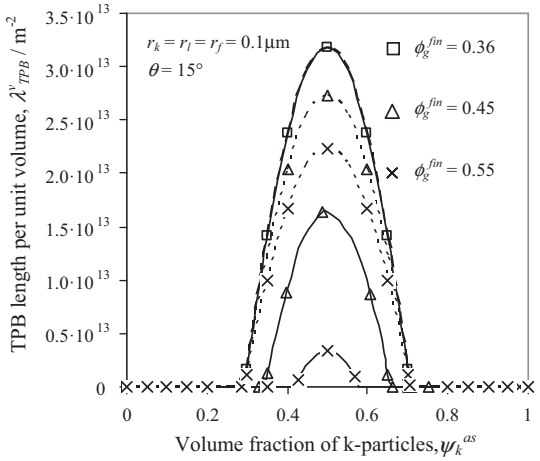

Fig. 4. TPB length per unit volume vs composition at different porosities for monosized particles: comparison between our model (solid lines) and other models (dotted lines) [9,14], in which pore formers do not affect numbers of contacts ($r_k = r_l = r_f = 0.1\,\mu m$, $\theta = 15°$).

porosity is considered constant and equal to 0.36 for each case. When porosity or composition of the bigger particles (l- in this case) increase, also R_h increases.

3.3. Pore formers size

The dimension of pore former particles, i.e. r_f, is another important parameter. Given the final porosity equal to 0.45 (i.e. fixed $\psi_f = 0.140625$) with initial porosity equal to 0.36 and kept constant, the radius r_f is varied in a ternary mixture of not polydisperse particles for the case $r_k = r_l = 0.1\,\mu m$. Fig. 6 shows that when r_f decreases, smaller f-particles surround k- and l-particles isolating them, i.e. breaking k-l, k-k and l-l contacts, resulting in lower λ^v_{TPB} and narrower ranges of composition where $\lambda^v_{TPB} > 0$. In this way, Fig. 6 suggests to use big pore former particles to increase the TPB length. Nevertheless, we must remember the limits of our model as described in Section 2.2: in order to apply the percolation model, the structure shall not collapse during the sintering, situation guaranteed by choosing pore former particles with proper size, i.e. similar to that of k- and l-particles. Thus, extremely fine or coarse pore former particles should be avoided. Instead, pore for-

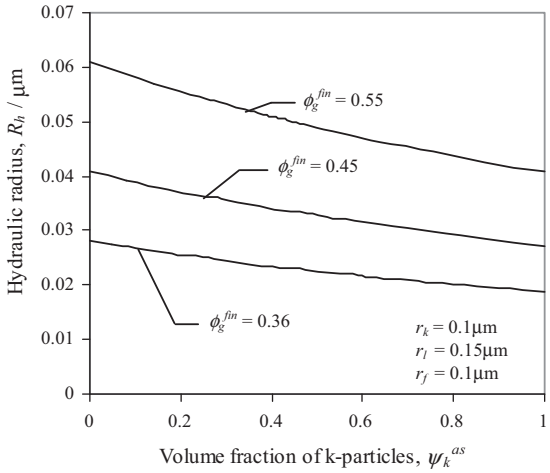

Fig. 5. Mean hydraulic radius as a function of k-particle volumetric composition for different final porosities obtained by using pore formers ($r_k = 0.1\,\mu m$, $r_l = 0.15\,\mu m$, $r_f = 0.1\,\mu m$).

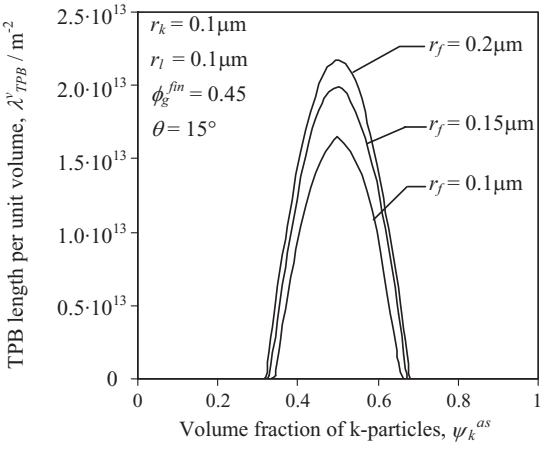

Fig. 6. Effect of the radius of pore formers on the TPB length per unit volume obtained after sintering for a monosized mixture ($r_k = r_l = 0.1$ μm, $\phi_g^{fin} = 0.45$, $\theta = 15°$): smaller pore former particles surround and isolate other particles resulting in a decrease of TPB length.

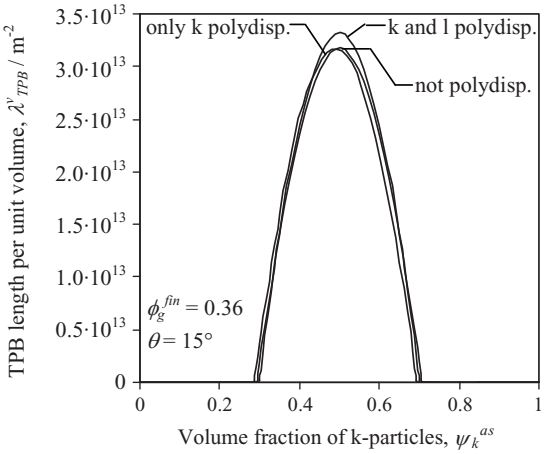

Fig. 8. TPB length per unit volume predicted for monosized and polydisperse mixtures: symmetrical volumetric distribution ($\phi_g^{fin} = 0.36$, $\theta = 15°$, $\bar{r}_k = \bar{r}_l = 0.1$ μm).

mers dimension should be close to the mean dimension of k- and l-particles or a bit bigger.

3.4. Polydisperse powders

Concerning polydisperse mixtures, in the case where pore formers are not used (i.e. we expect final porosity of about 0.36) with $\theta = 15°$, we compare the TPB length per unit volume as a function of composition after sintering among monosized and polydisperse mixtures.

To describe polydisperse powders, a symmetrical numerical dispersion is considered as follows (described for k-particles, for l-particles it is the same):

$$\begin{cases} r_{k1} = \bar{r}_k - 0.4 \cdot \bar{r}_k & \zeta_{k1} = 0.1 \cdot \zeta_k \\ r_{k2} = \bar{r}_k - 0.2 \cdot \bar{r}_k & \zeta_{k2} = 0.2 \cdot \zeta_k \\ r_{k3} = \bar{r}_k & \zeta_{k3} = 0.4 \cdot \zeta_k \\ r_{k4} = \bar{r}_k + 0.2 \cdot \bar{r}_k & \zeta_{k4} = 0.2 \cdot \zeta_k \\ r_{k5} = \bar{r}_k + 0.4 \cdot \bar{r}_k & \zeta_{k5} = 0.1 \cdot \zeta_k \end{cases} \quad (32)$$

while a monosized powder is merely represented by its numerical fraction (e.g. ζ_k) and radius (e.g. r_k).

Fig. 7 shows the effect of the numerical dispersion on λ^v_{TPB} for $\bar{r}_k = \bar{r}_l = 0.1$ μm. When a phase is polydisperse it behaves as it was made of bigger particles, since in a symmetrical numerical distribution the major contribution in the determination of numbers of contacts and probabilities of connection is due to bigger particles. Fig. 7 can also be read in a different way: if polydisperse powders were considered as monosized powders, the TPB length would be overestimated of about 25%. Similar results and considerations are also reported by Kenney et al. [11], who used computer simulations to evaluate λ^v_{TPB}.

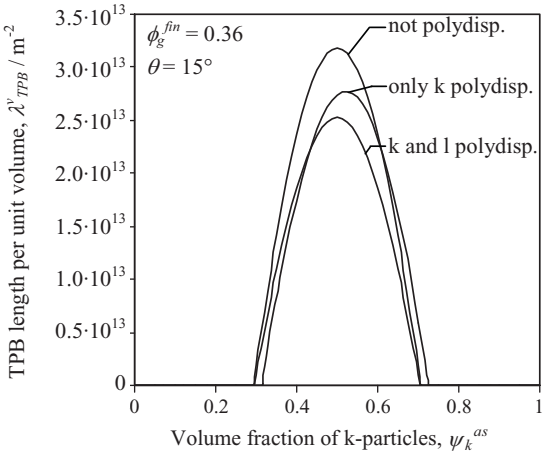

Fig. 7. TPB length per unit volume predicted for monosized and polydisperse mixtures: symmetrical numerical distribution ($\phi_g^{fin} = 0.36$, $\theta = 15°$, $\bar{r}_k = \bar{r}_l = 0.1$ μm).

In Fig. 8 a symmetrical volumetric distribution, equal to the numerical distribution described in system (32), is used (i.e. numerical fractions ζ_{ki} and ζ_k are replaced with volume fractions ψ_{ki} and ψ_k). Fig. 8 shows little differences between monosized and polydisperse mixtures because the effects of bigger particles of the distribution are balanced by smaller particles that have the same volume fraction. In this situation the errors that we will make on the estimation of λ^v_{TPB} considering monosized particles instead of polydisperse mixtures are low, but this is principally due to the fact that the volumetric dispersion is symmetrical. Thus, for a generic volumetric dispersion (i.e. not symmetrical) it is reasonable that the estimation of λ^v_{TPB} will be more accurate if we consider that distribution instead of using a mean particle diameter for each phase.

4. Conclusions

A percolation model has been developed to predict effective properties of composite electrodes for SOFCs (such as TPB length per unit volume and mean hydraulic radius) from controllable powder characteristics such as particle size distributions and compositions. Such effective properties are needed to assist the design and optimization of electrode structures by continuum-based mathematical models. The proposed model extends percolation theory to multicomponent polydisperse mixtures. As a consequence the actual granulometric distribution of powders may be implemented in the model. Simulations show that morphological properties of the resulting packing depend on the granulometric distribution of the powders. Predicted results may vary considerably if the actual granulometric distribution of the powders is used instead of the mean particle dimension, in particular for asymmetrical or wide particle distributions, suggesting that polydispersion of particles must be considered in SOFC electrode models.

Another feature introduced by the model is the extension of the theory to account for pore former particles (i.e. porosity), which enables the estimation of functional properties by the knowledge of the amount of pore formers introduced before sintering. Effective

properties are strongly influenced by the variation of volume fraction of pore formers, which affects both numbers of contacts (i.e. probabilities of connection) and number of particles per unit volume after sintering. The first effect is generally neglected in other percolation theories resulting in particular in an overestimation of TPB length. This approach may be implemented for systems in which the cell design must be expressly studied to keep the mass transfer limitations to a minimum [30].

The model can then be considered a valuable tool for the structural design of electrodes, since it provides a quantitative connection between measurable and effective functional characteristics.

Acknowledgements

This effort was supported by the National Research Council - Institute of Energetics and Interphases, under the research grant "Modeling of protonic-anionic mixed conduction membranes for fuel cells and electrolyzers".

References

[1] A. Barbucci, M. Carpanese, A.P. Reverberi, G. Cerisola, M. Blanes, P.L. Cabot, M. Viviani, A. Bertei, C. Nicolella, J. Appl. Electrochem. 38 (2008) 939–945.
[2] P. Costamagna, M. Panizza, G. Cerisola, A. Barbucci, Electrochim. Acta 47 (2002) 1079–1089.
[3] B. Kenney, K. Karan, Solid State Ionics 178 (2007) 297–306.
[4] H. Zhu, R.J. Kee, J. Electrochem. Soc. 155 (2008) B715–B729.
[5] J.R. Wilson, A.T. Duong, M. Gameiro, H.Y. Chen, K. Thornton, D.R. Mumm, S.A. Barnett, Electrochem. Commun. 11 (2009) 1052–1056.
[6] J.R. Wilson, W. Kobsiriphat, R. Mendoza, H.Y. Chen, J.M. Hiller, D.J. Miller, K. Thornton, P.W. Voorhees, S.B. Adler, S.A. Barnett, Nature 5 (2006) 541–544.
[7] Y. Suzue, N. Shikazono, N. Kasagi, J. Power Sources 184 (2008) 52–59.
[8] J.H. Nam, D.H. Jeon, Electrochim. Acta 51 (2006) 3446–3460.
[9] P. Costamagna, P. Costa, V. Antonucci, Electrochim. Acta 43 (1998) 375–394.
[10] C. Nicolella, A. Bertei, M. Viviani, A. Barbucci, J. Appl. Electrochem. 39 (2009) 503–511.
[11] B. Kenney, M. Valdmanis, C. Baker, J.G. Pharoah, K. Karan, J. Power Sources 189 (2009) 1051–1059.
[12] I.V. Belova, G.E. Murch, J. Phys. Chem. Solids 66 (2005) 722–728.
[13] R. Al-Raoush, M. Alsaleh, Powder Technol. 176 (2007) 47–55.
[14] D. Chen, Z. Lin, H. Zhu, R.J. Kee, J. Power Sources 191 (2009) 240–252.
[15] M. Suzuki, T. Oshima, Powder Technol. 35 (1983) 159–166.
[16] D. Bouvard, F.F. Lange, Acta Metall. Mater. 39 (1991) 3083–3090.
[17] A. Bertei, C. Nicolella, Powder Technol., in press, doi:10.1016/j.powtec.2011.07.011.
[18] D. Dong, J. Gao, X. Liu, G. Meng, J. Power Sources 165 (2007) 217–223.
[19] L. Bi, Z. Tao, W. Sun, S. Zhang, R. Peng, W. Liu, J. Power Sources 191 (2009) 428–432.
[20] K. Howe, G.J. Thompson, K. Kendall, J. Power Sources 196 (2011) 1677–1686.
[21] C. Jin, J. Liu, L. Li, Y. Bai, J. Membr. Sci. 341 (2009) 233–237.
[22] C.H. Kuo, P.K. Gupta, Acta Metall. Mater. 43 (1995) 397–403.
[23] J.H. Yu, G.W. Park, S. Lee, S.K. Woo, J. Power Sources 163 (2007) 926–932.
[24] G.D. Scott, Nature (London) 188 (1960) 908–909.
[25] W.S. Jodrey, E.M. Tory, Powder Technol. 30 (1981) 111–118.
[26] G.T. Nolan, P.E. Kavanagh, Powder Technol. 72 (1992) 149–155.
[27] R. Ben Aim, P. Le Goff, Powder Technol. 1 (1967) 281–290.
[28] V.M. Janardhanan, V. Heuveline, O. Deutschmann, J. Power Sources 178 (2008) 368–372.
[29] R.B. Bird, W.E. Steward, E.N. Lightfoot, Transport Phenomena , John Wiley and Sons, New York, 1960, p. 197.
[30] S. Kjelstrup, M.-O. Coppens, J.G. Pharoah, P. Pfeifer, Energy Fuels 24 (2010) 5097–5108.

Glossary

a_k^v: surface area exposed by k-particles to gas phase per unit volume (m^{-1})
a_{kl}^v: contact area between connected k- and l-particles per unit volume (m^{-1})
a_l^v: surface area exposed by l-particles to gas phase per unit volume (m^{-1})
m_h: number of particle sizes for a type of particles (h = k, l or f)
n^v: number of particles per unit volume (voids included) (m^{-3})
p: probability of connection of a type of particles
P: ratio of radii of particles
P_{max}: maximum ratio of radii to avoid segregation
P_{min}: minimum ratio of radii to avoid segregation
r: radius of a type of particles (m)
R_h: mean hydraulic radius (m)
S: surface area fraction of a type of particles
V: volume of a particle (m^3)
$Z_{h,h}$: overall average number of contacts for all h-particles (h = k, l or f)
Z_{hi}: average coordination number of hi-particles (h = k, l or f)
$Z_{hi,f}$: average number of contacts between a hi-particle and f-particles
$Z_{hi,g}$: average number of contacts between a hi-particle and g-particles
$Z_{hi,gj}$: average number of contacts between a hi-particle and gj-particles
$Z_{hi,gj}\big|_{\zeta_{gj}\to 1}$: limit average number of contacts of a hi-particle with gj-particles
$Z_{hi,k}$: average number of contacts between a hi-particle and k-particles
$Z_{hi,l}$: average number of contacts between a hi-particle and l-particles
Z_k: average coordination number of k-particles
$Z_{k,k}$: overall average number of contacts for all k-particles
Z_l: average coordination number of l-particles
$Z_{l,l}$: overall average number of contacts for all l-particles
ζ: numerical fraction of a type of particles
θ: mean contact angle between two particles (rad)
λ_{TPB}^v: three-phase boundary length per unit volume (m^{-2})
ϕ_g^f: fraction of porosity created by pore formers
ϕ_g^{fin}: final porosity (after sintering)
ϕ_g^{in}: initial porosity (before sintering)
ψ: volume fraction of a type of particles relative to the total solid

Superscripts

as: after sintering
bs: before sintering
c: circle of contact
eff: effective
kk: k-k contact
kl: k-l contact
lk: l-k contact
ll: l-l contact
lost: lost in contacts
overlap: overlapping effects considered

Subscripts

f: pore former particles
fi: i-th pore former particle size
g: g-particles (g = k, l or f if not otherwise specified)
gj: j-th g-particle size (g = k, l or f if not otherwise specified)
h: h-particles (h = k, l or f if not otherwise specified)
hi: i-th h-particle size (h = k, l or f if not otherwise specified)
k: k-particles
ki: i-th k-particle size
kk: k-k contact
kl: k-l contact
l: l-particles
li: i-th l-particle size
lk: l-k contact
ll: l-l contact